

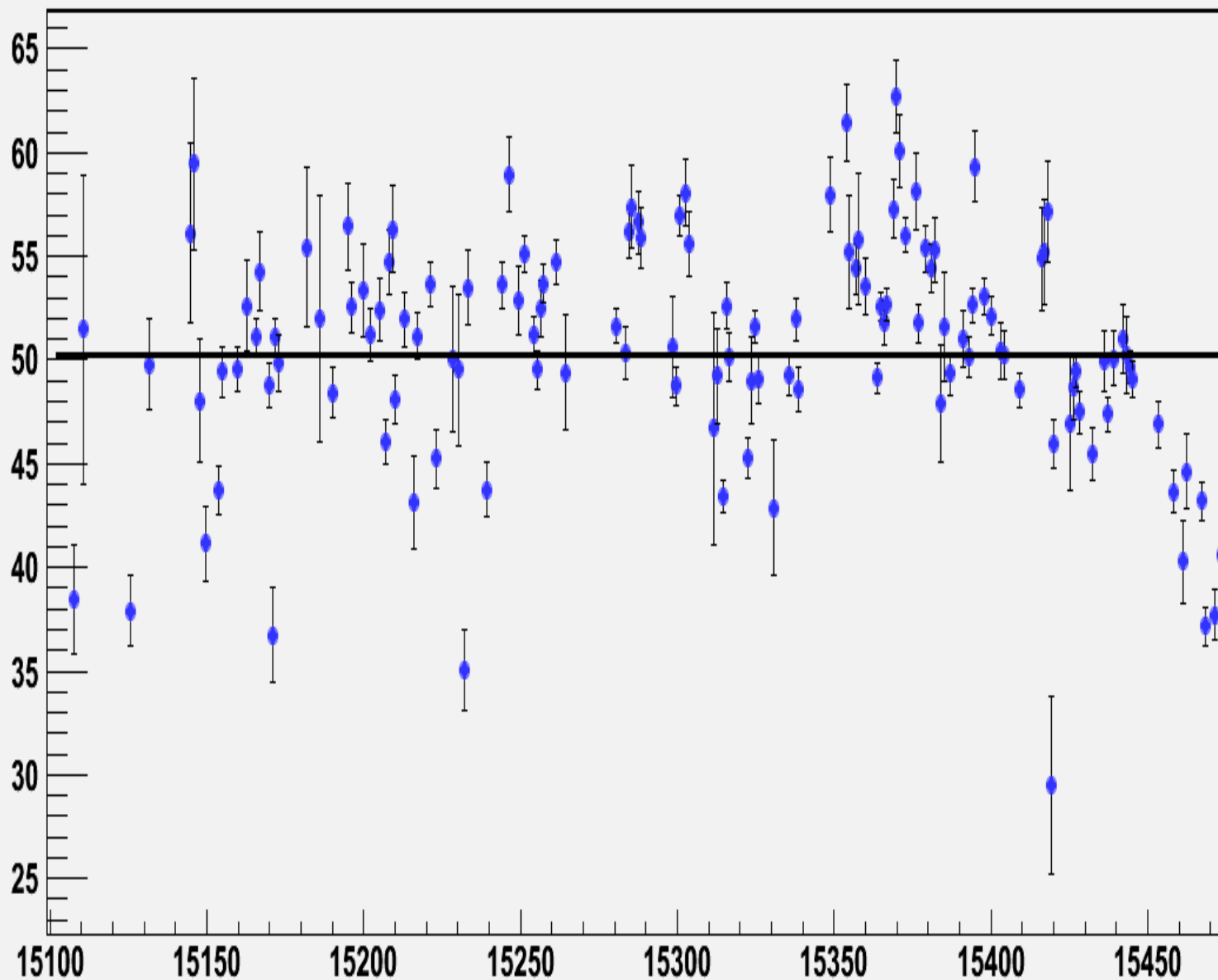
Precision P-P CNI polarimeter for RHIC
with molecular (un-polarized) hydrogen
jet target.

A. Zelenski

SPIN Meeting, October 12, 2011

Blue-1, 250 GeV, Run-2011

Polarization, %

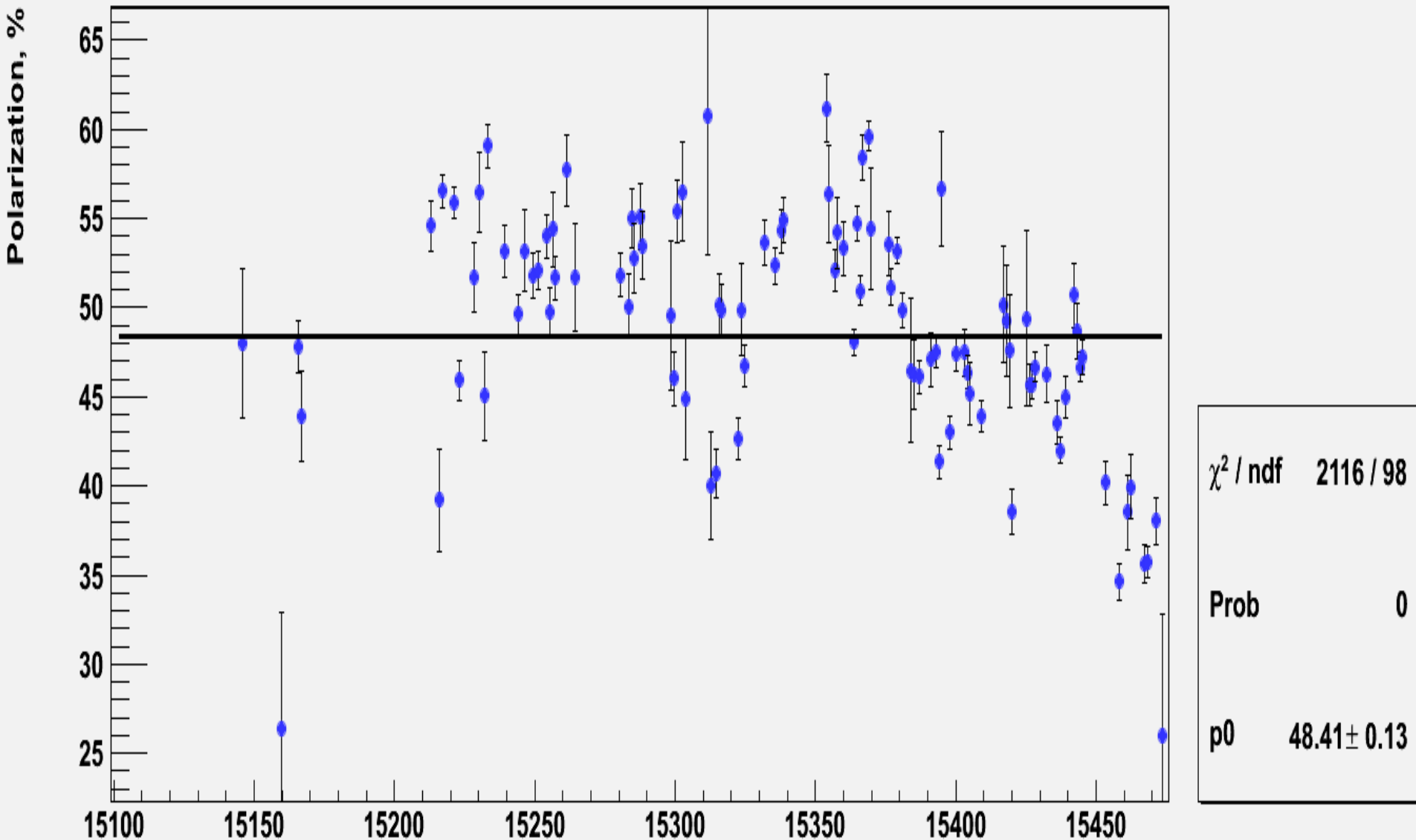


χ^2 / ndf 1739 / 129

Prob 0

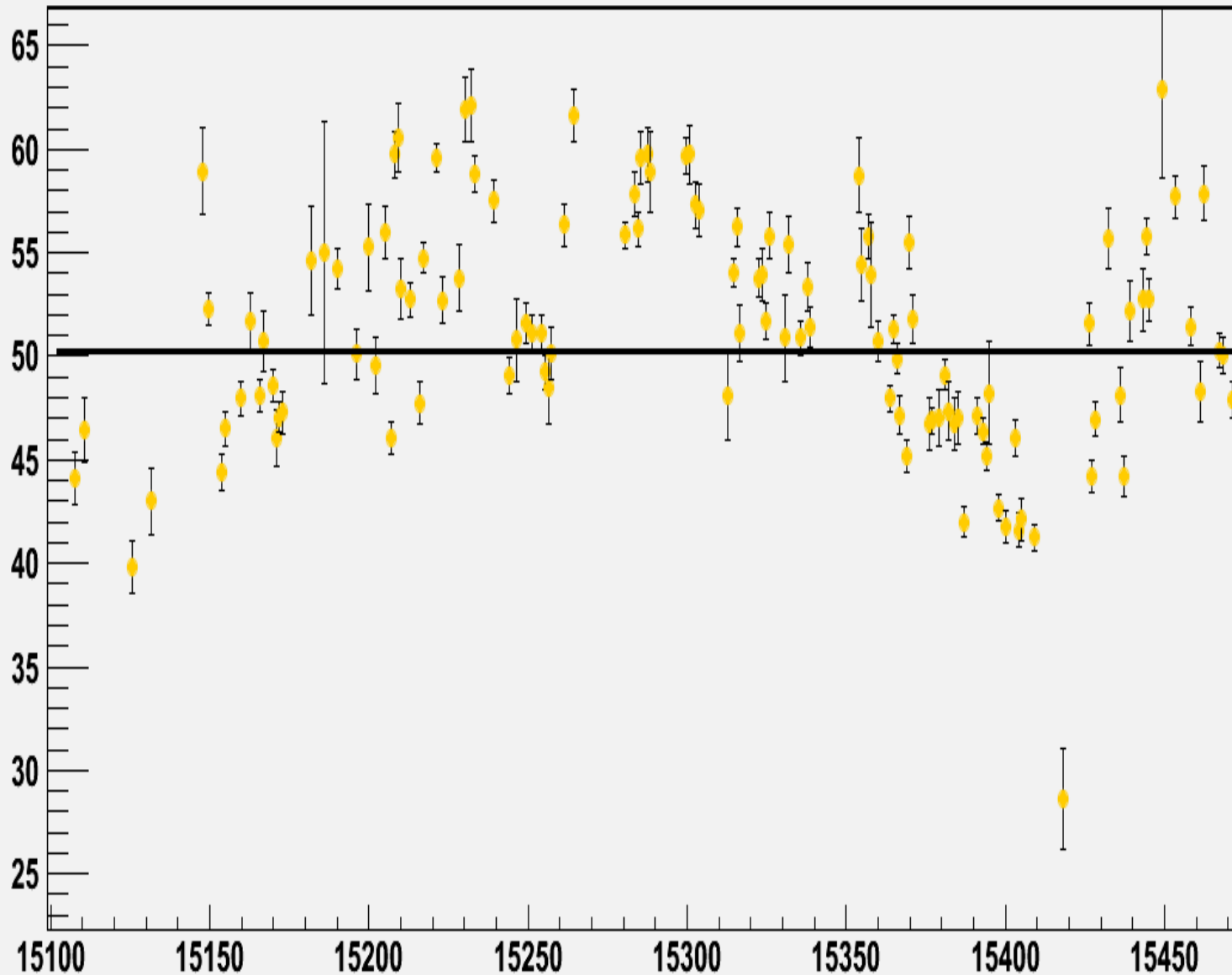
p0 50.28 ± 0.11

Blue-2, Vertical target, 250 GeV



Yellow-2, 250 GeV, Run-2011

Polarization, %



χ^2 / ndf 3222 / 119

Prob 0

p0 50.27 ± 0.09

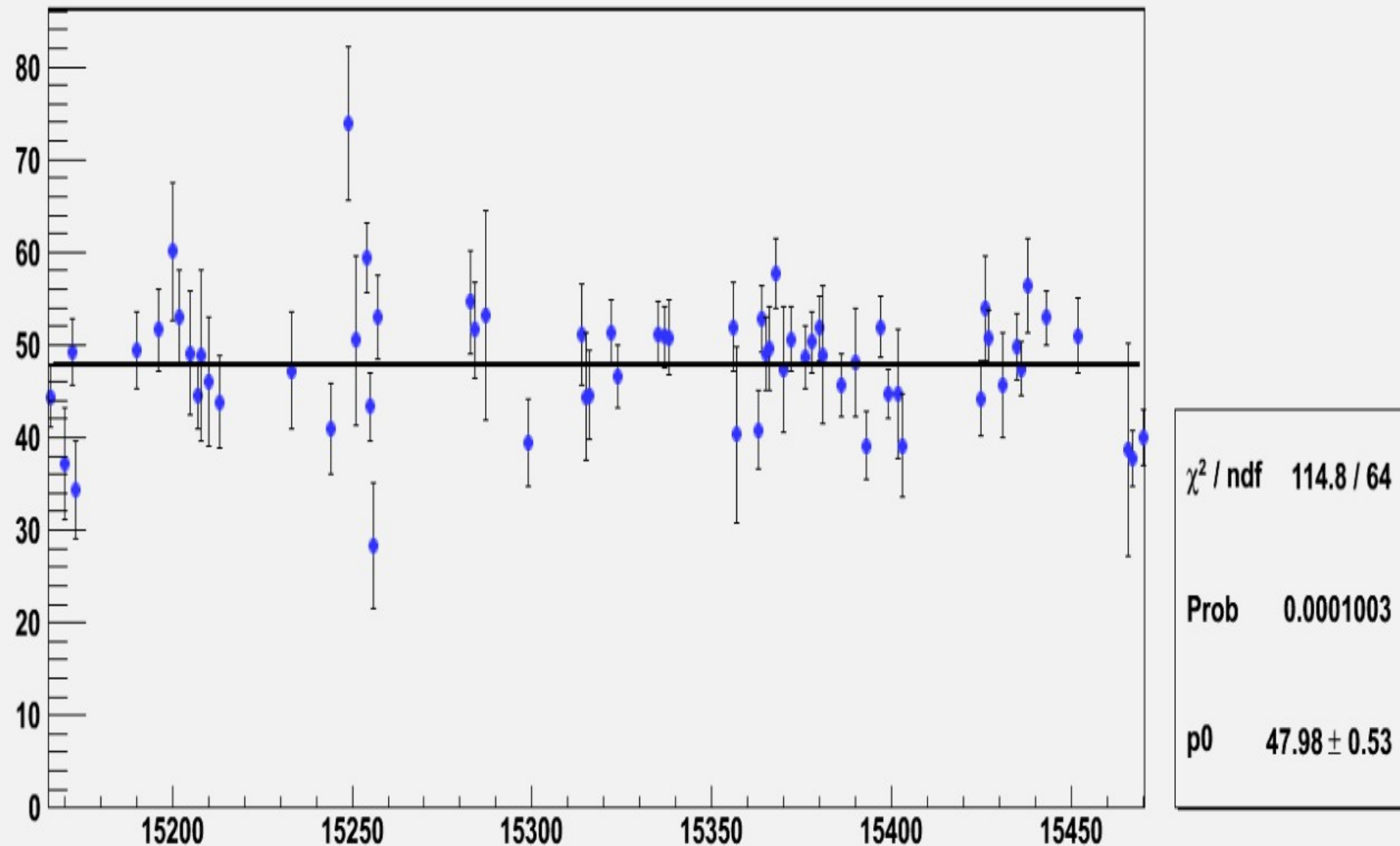
Measurements with the p-Carbon polarimeter.

15431.003	Apr 10, 2011 13:31:47 Sun	B1U	39.9 ± 1.7	0.13 ± 0.12	sweep	249.73
15431.303	Apr 10, 2011 13:28:20 Sun	Y2U	51.9 ± 2.0	0.25 ± 0.11	sweep	249.73
15431.203	Apr 10, 2011 13:27:34 Sun	B2D	44.5 ± 2.2	0.13 ± 0.11	sweep	249.73
15431.002	Apr 10, 2011 13:07:55 Sun	B1U	46.8 ± 1.7	0.20 ± 0.11	sweep	249.73
15431.302	Apr 10, 2011 13:05:35 Sun	Y2U	55.2 ± 1.9	0.28 ± 0.11	sweep	249.73
15431.202	Apr 10, 2011 13:05:19 Sun	B2D	44.4 ± 2.4	0.29 ± 0.18	sweep	249.73

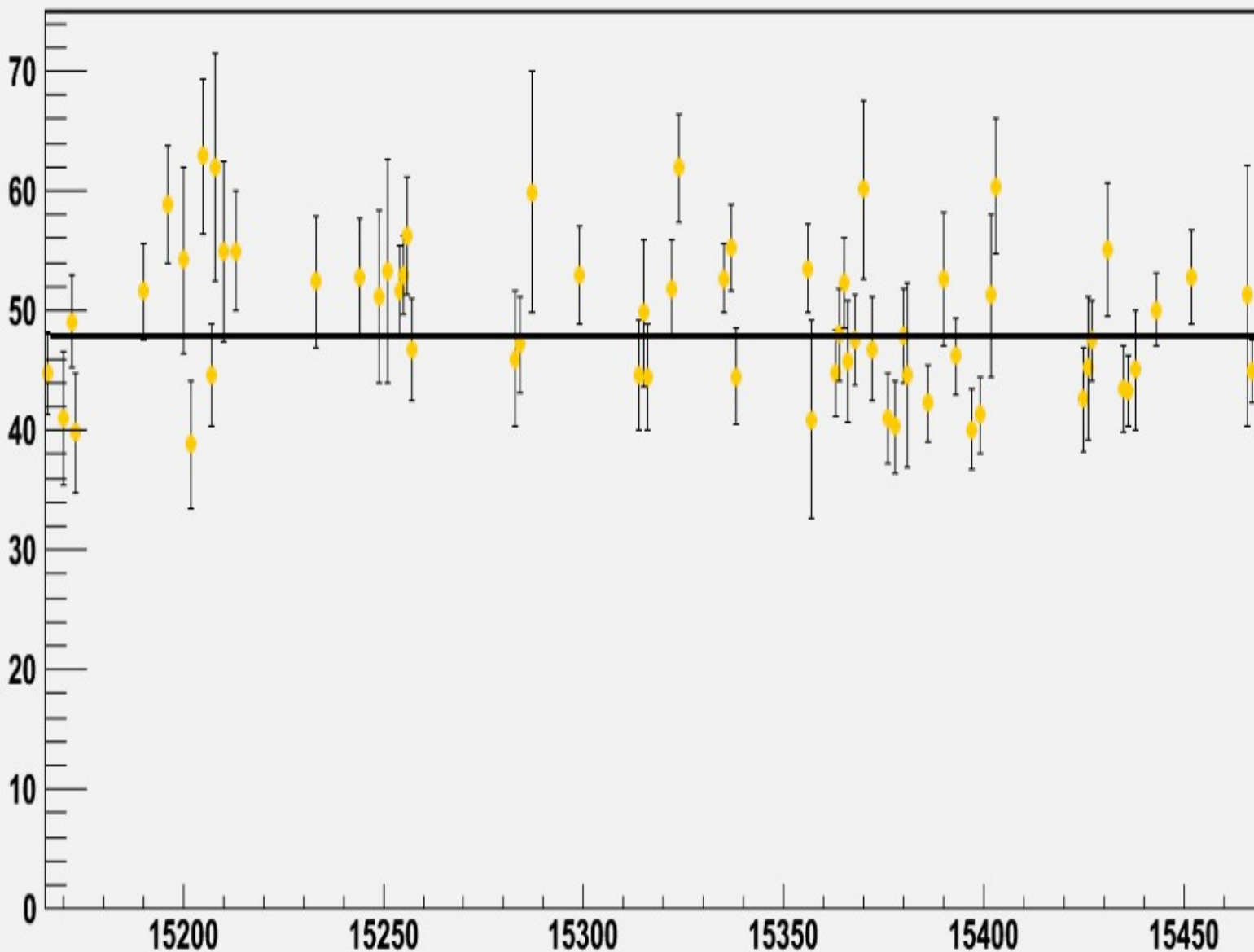
Measurements with the p-Carbon polarimeter in 2011.

15427.008	Apr 10, 2011 05:25:16 Sun	B1U	48.6 ± 2.3	-0.31 ± 0.14	sweep	249.73	H6
15427.007	Apr 10, 2011 05:24:22 Sun	B1U	40.8 ± 4.1	0.02 ± 0.21	sweep	249.73	H6
15427.208	Apr 10, 2011 05:22:39 Sun	B2D	52.6 ± 2.3	-0.32 ± 0.18	sweep	249.73	V6
15427.308	Apr 10, 2011 05:22:08 Sun	Y2U	46.7 ± 2.3	0.19 ± 0.33	fixed	249.73	H1
15427.307	Apr 10, 2011 05:21:16 Sun	Y2U	48.7 ± 10.3	0.68 ± 0.63	sweep	249.73	H1
15427.207	Apr 10, 2011 05:21:16 Sun	B2D	44.1 ± 7.2	0.32 ± 0.46	sweep	249.73	V6
15427.006	Apr 10, 2011 05:18:22 Sun	B1U	41.6 ± 1.7	0.55 ± 0.22	sweep	249.73	H6
15427.306	Apr 10, 2011 05:15:21 Sun	Y2U	37.0 ± 1.8	0.74 ± 0.19	sweep	249.73	H1
15427.206	Apr 10, 2011 05:15:07 Sun	B2D	41.8 ± 1.7	-0.00 ± 0.09	sweep	249.73	V6
15427.005	Apr 10, 2011 03:23:40 Sun	B1U	48.1 ± 1.8	0.16 ± 0.15	sweep	249.73	H6
15427.305	Apr 10, 2011 03:21:12 Sun	Y2U	41.7 ± 1.9	0.34 ± 0.16	sweep	249.73	H1
15427.205	Apr 10, 2011 03:20:53 Sun	B2D	42.2 ± 1.8	0.24 ± 0.11	sweep	249.73	V6
15427.004	Apr 10, 2011 00:22:59 Sun	B1U	47.2 ± 1.8	0.17 ± 0.11	sweep	249.73	H6

H-jet, Blue beam, 250 GeV, Run-2011



H-jet, Yellow beam, 250 GeV, Run 2011



χ^2 / ndf 106 / 64

Prob 0.000756

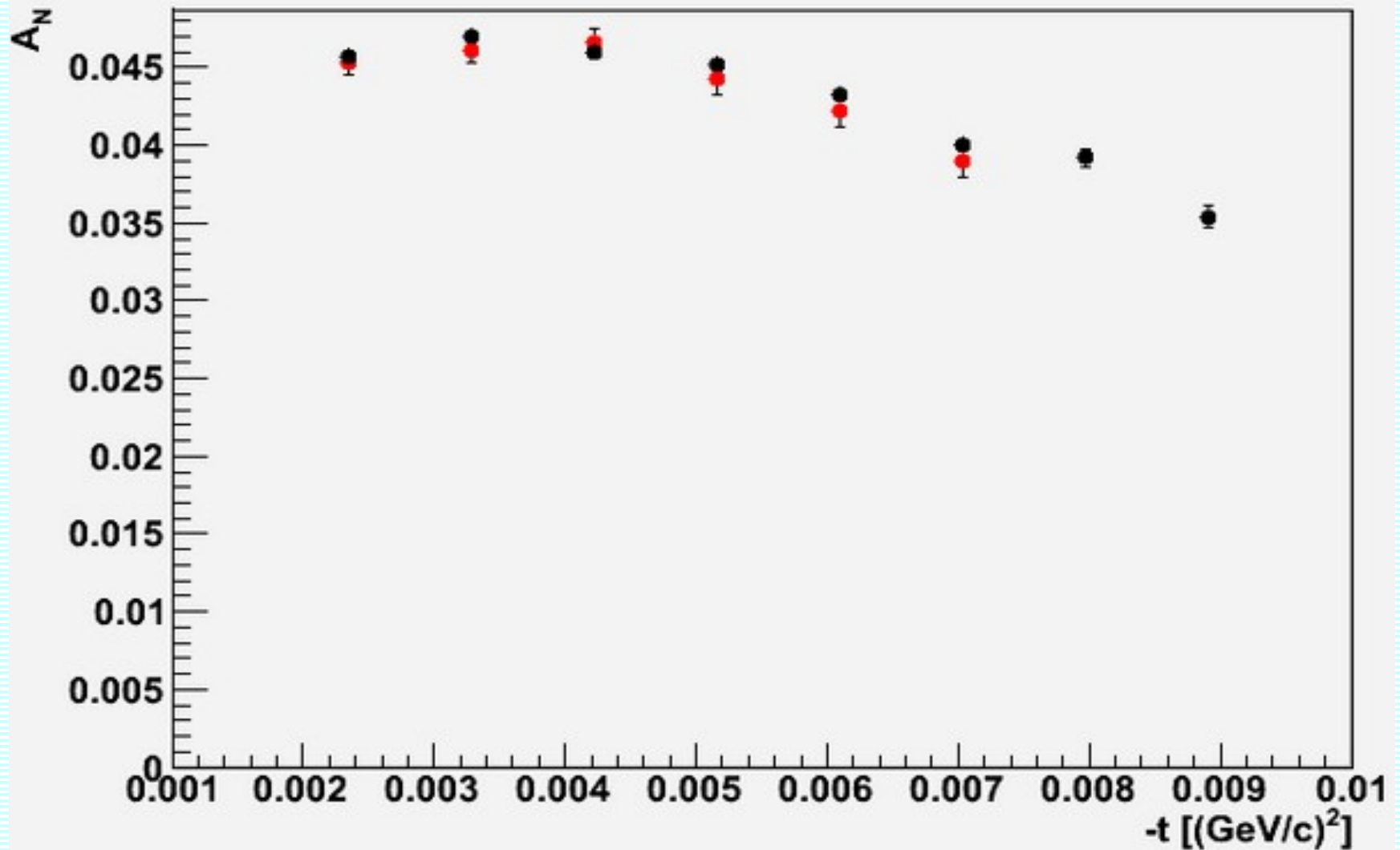
p0 47.95 ± 0.53

H-jet polarimeter measurements in Run 2011.

15393	0.0461 +- 0.0014	0.4624 +- 0.0315	0.0404 +- 0.0017	0.3908 +- 0.0370
15397	0.0441 +- 0.0014	0.4008 +- 0.0325	0.0443 +- 0.0015	0.5187 +- 0.0327
15399	0.0418 +- 0.0014	0.4134 +- 0.0319	0.0437 +- 0.0012	0.4469 +- 0.0274
15402	0.0449 +- 0.0030	0.5126 +- 0.0678	0.0425 +- 0.0031	0.4470 +- 0.0693
15403	0.0413 +- 0.0025	0.6038 +- 0.0563	0.0392 +- 0.0025	0.3912 +- 0.0560
15425	0.0429 +- 0.0019	0.4256 +- 0.0430	0.0387 +- 0.0019	0.4420 +- 0.0409
15426	0.0391 +- 0.0027	0.4518 +- 0.0599	0.0417 +- 0.0025	0.5386 +- 0.0563
15427	0.0426 +- 0.0015	0.4750 +- 0.0327	0.0432 +- 0.0014	0.5069 +- 0.0305
15431	0.0452 +- 0.0025	0.5515 +- 0.0563	0.0451 +- 0.0026	0.4558 +- 0.0574
15435	0.0454 +- 0.0016	0.4342 +- 0.0365	0.0459 +- 0.0016	0.4982 +- 0.0358
15436	0.0429 +- 0.0013	0.4328 +- 0.0301	0.0452 +- 0.0013	0.4738 +- 0.0293
15438	0.0435 +- 0.0022	0.4510 +- 0.0499	0.0455 +- 0.0023	0.5637 +- 0.0506
15443	0.0457 +- 0.0014	0.5009 +- 0.0311	0.0448 +- 0.0014	0.5292 +- 0.0302
15452	0.0430 +- 0.0018	0.5279 +- 0.0387	0.0458 +- 0.0019	0.5097 +- 0.0412
15466	0.0484 +- 0.0049	0.5127 +- 0.1090	0.0374 +- 0.0053	0.3861 +- 0.1154
15467	0.0443 +- 0.0011	0.4493 +- 0.0256	0.0434 +- 0.0014	0.3777 +- 0.0305
15470	0.0437 +- 0.0013	0.4263 +- 0.0289	0.0444 +- 0.0014	0.4005 +- 0.0306

$\Delta P/P \sim 6\text{-}7\%$ for one fill (statistical).

P-P elastic scattering analyzing power in CNI region.



Towards precision polarimetry in RHIC. Summary.

- Analyzing power of P-P elastic scattering in CNR region has been accurately measured in experiments with H-jet polarimeter in energy range 24-250 GeV.
- This accuracy can be further improved after studies of molecular H₂ background and other systematic errors contributions.
- The known analyzing power can be used in the polarimeter with higher thickness un-polarized H₂-jet target and 100 times higher counting rate.
- This will result in less than 1% statistical accuracy for each fill.
- Tenfold rate increase can be obtained due to Jet geometry optimization and detector solid angle increase.
- In this assumption, the required H₂-jet target thickness will be about:
$$(5-10) \cdot 10^{12} \text{ H}_2 \text{ molecules /cm}^2.$$
- This target thickness can be achieved in comparatively simple H₂-jet target.
- The effect of this Jet-target to the beam and RHIC vacuum will be small (comparable with the polarized H₂-jet target).

Supersonic gas jet target.

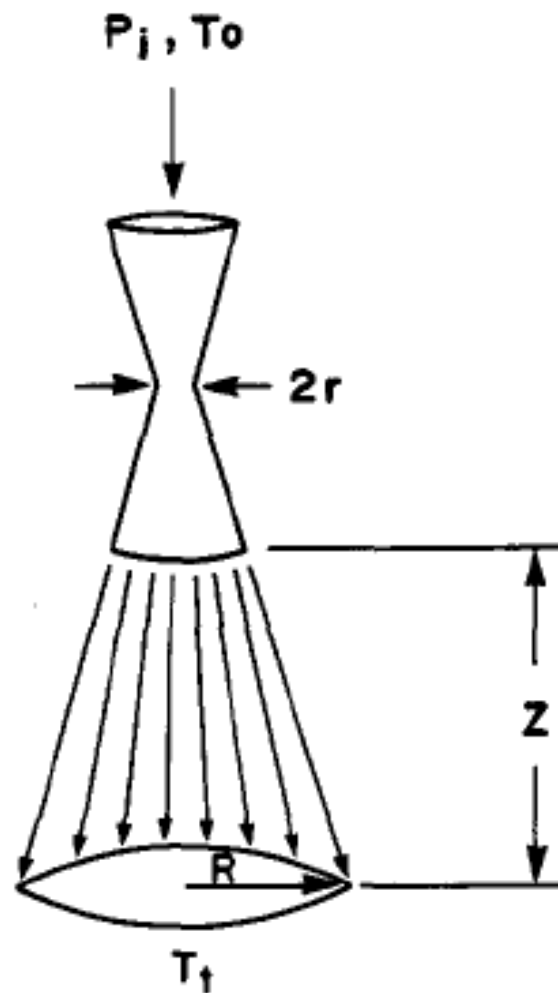


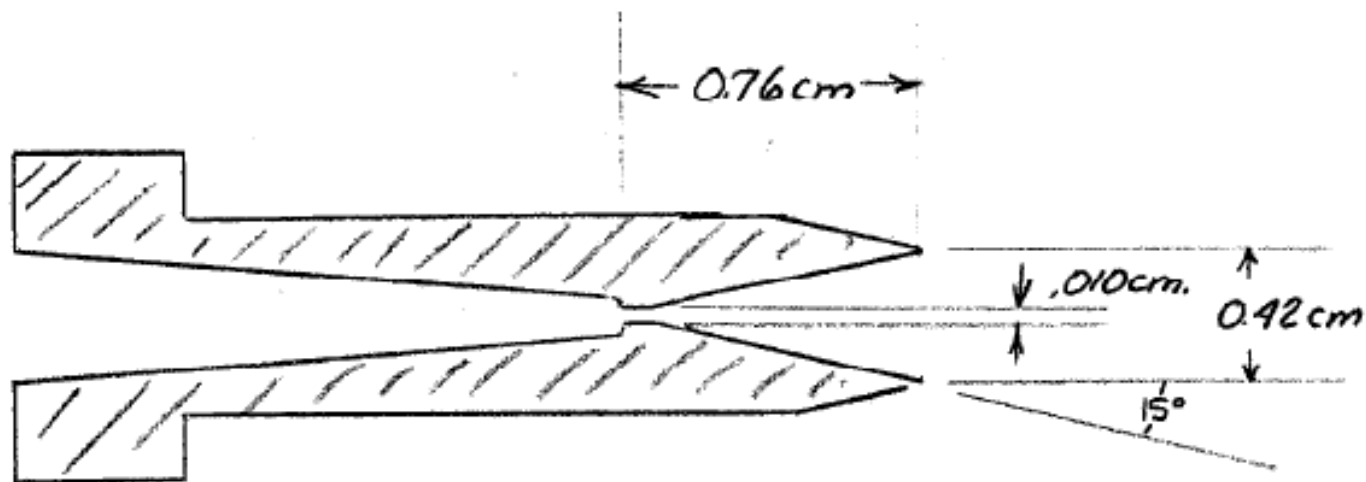
Fig. 1. Schematic of the de Laval nozzle and jet. P_i and T_0 are the input pressure and temperature in K of the target gas. Z is the length of the jet and R is its radius at beam intersection.

Nozzle geometry of the Jet target at FNAL.

5.1 The Nozzle Assembly

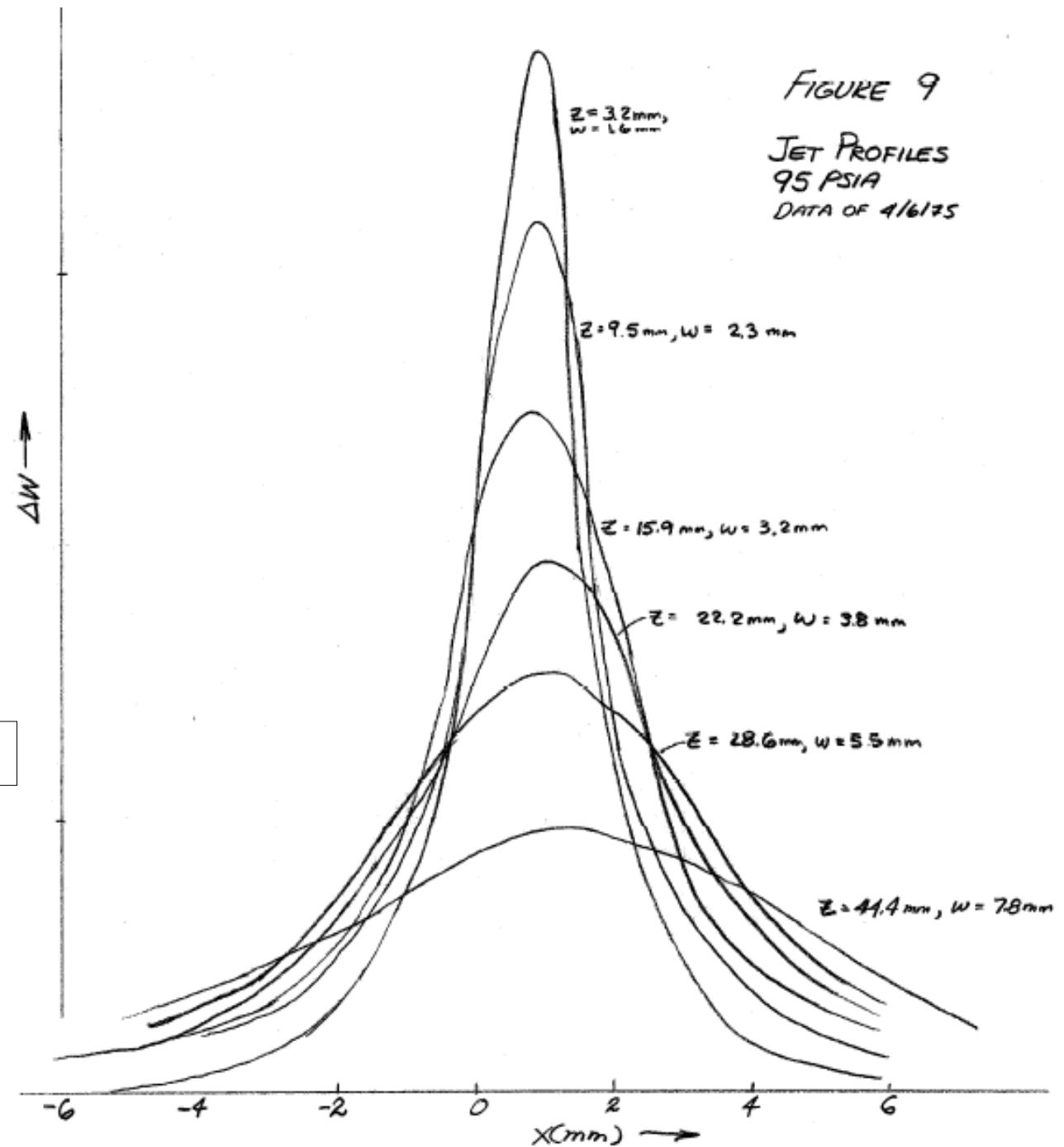
P.Mantcsh,. FNAL, TM-582

A continuous duty gas jet target was recently developed by Brolley⁴ for use at the LAMPF machine at Los Alamos. In the course of this work, techniques were devised for making de Laval type converging-diverging nozzles of very small throat diameter (.002 to .010 cm). The nozzle used in the present studies was provided by Brolley. A sketch of this nozzle and its dimensions are shown below:



THE LOS ALAMOS NOZZLE

H-jet profile vs. Z ,



P.Mantcsh,. FNAL, TM-582

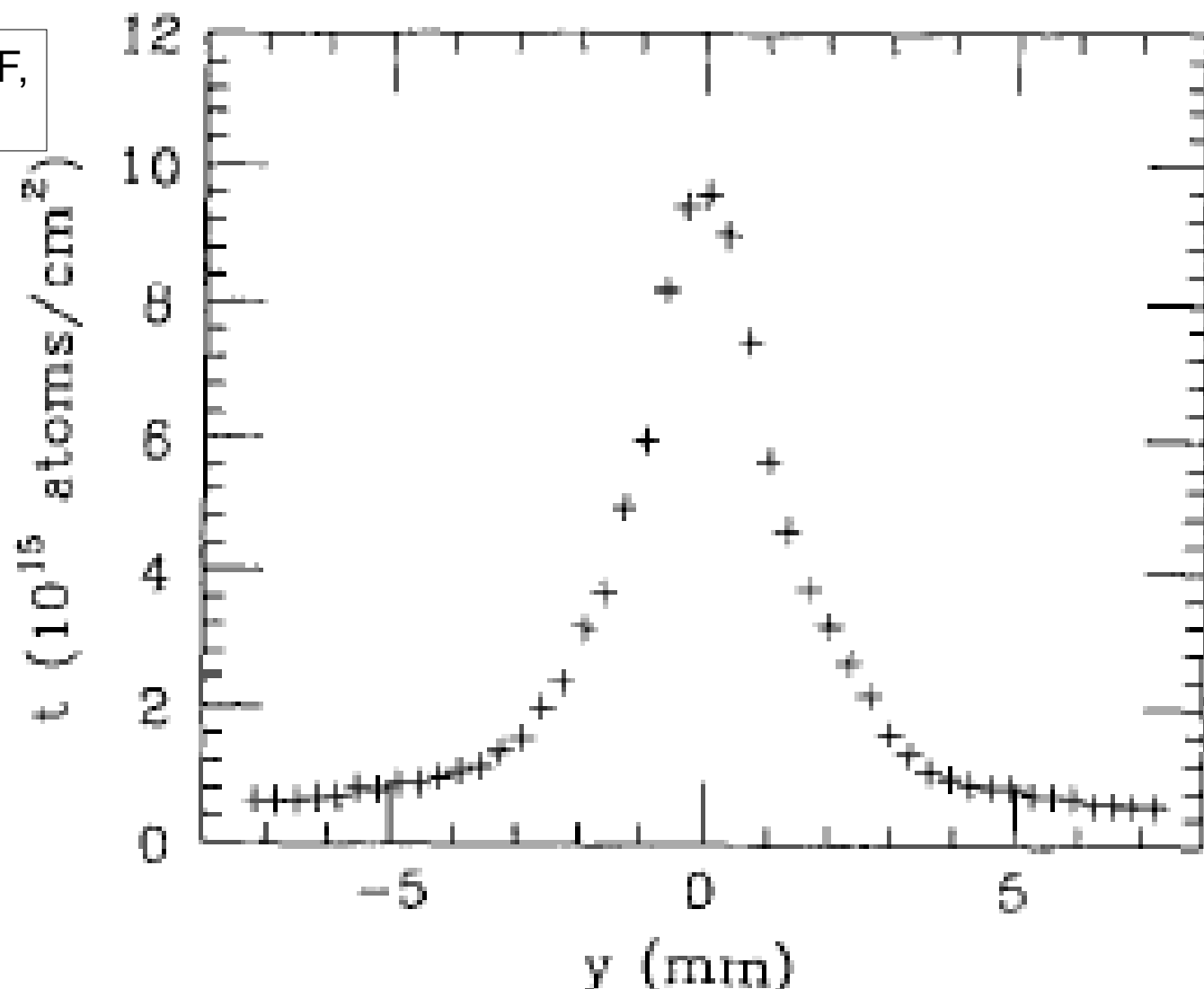
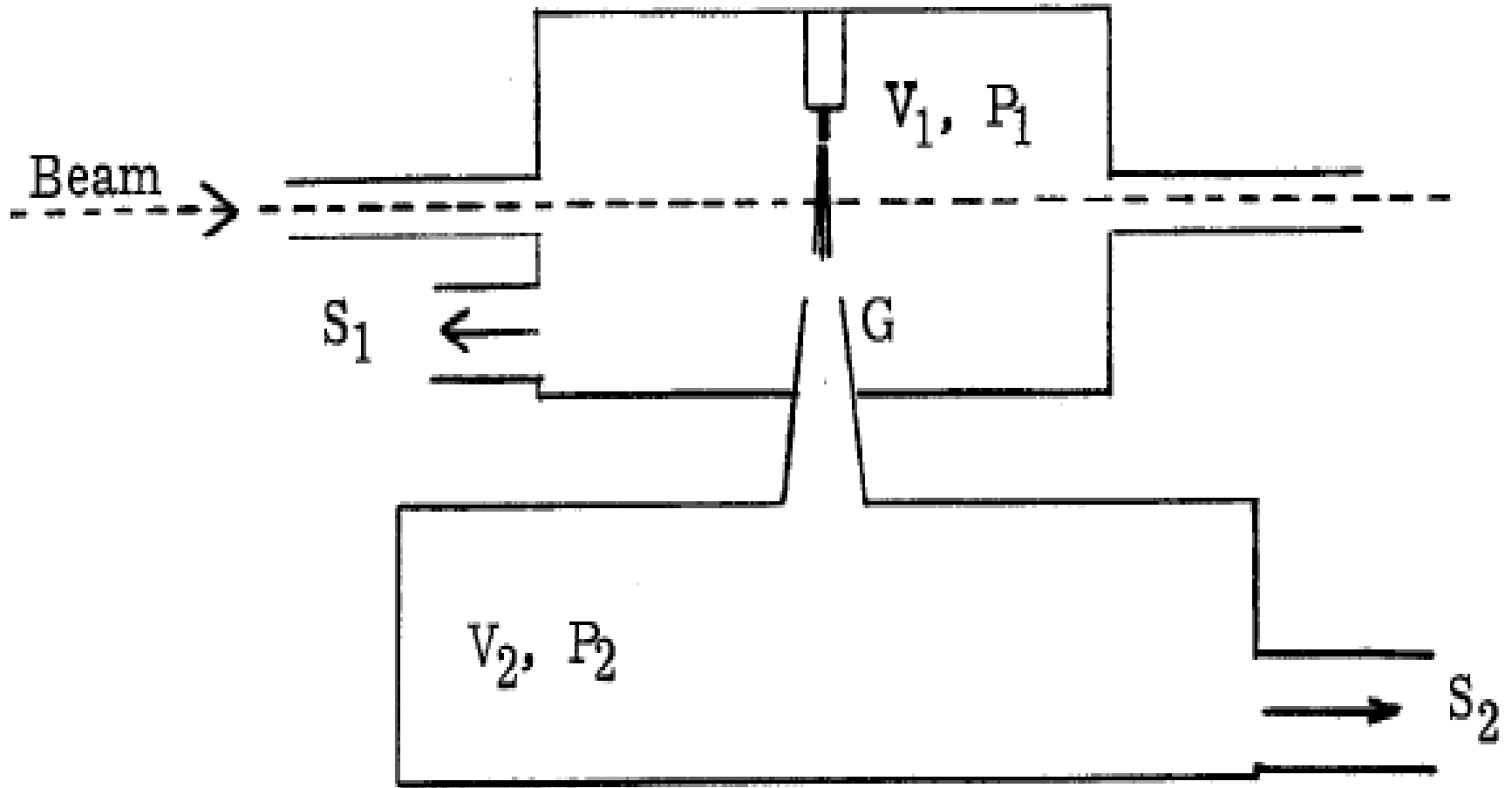
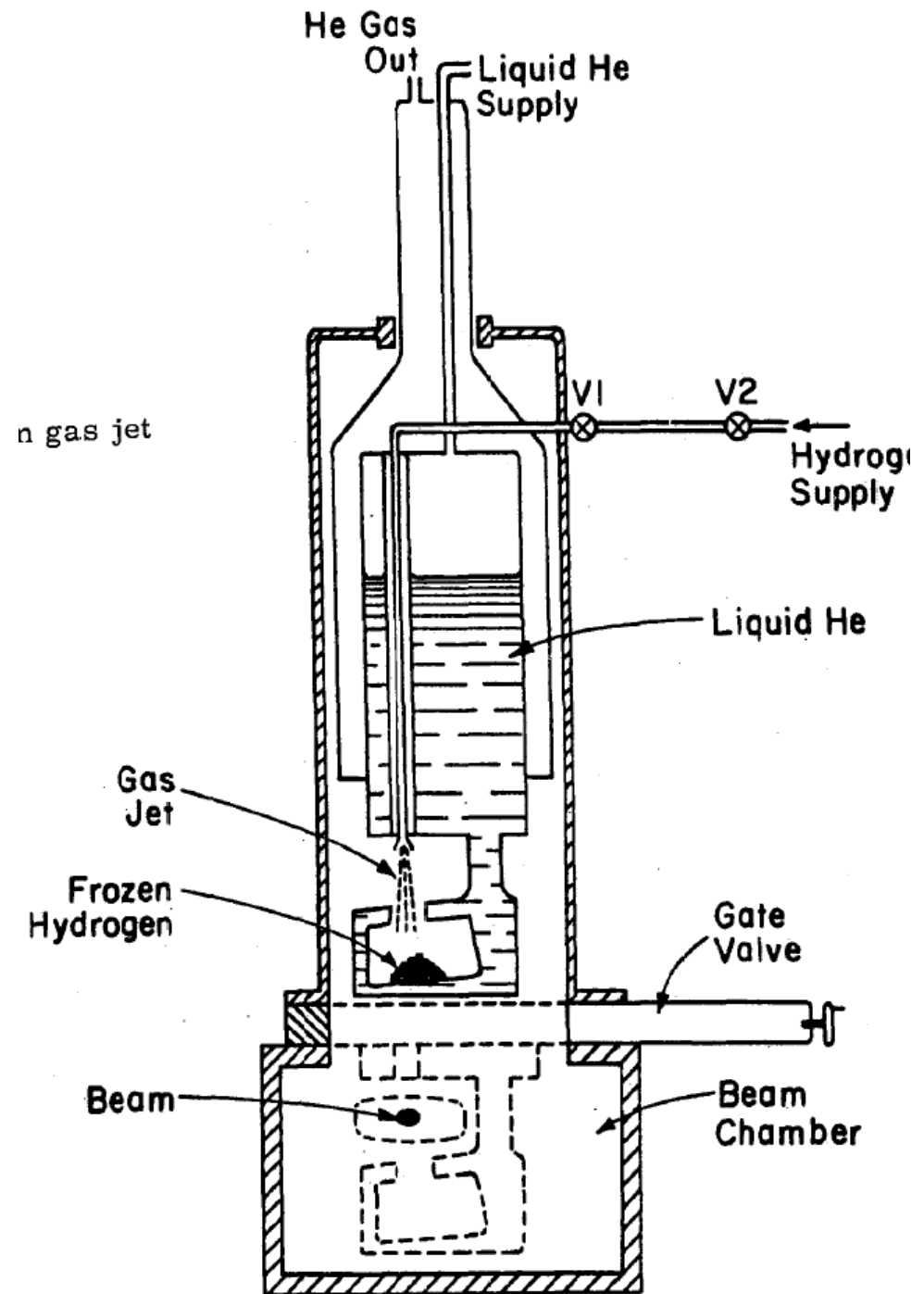


Fig. 5. Thickness profile of an H₂ jet from a 108 μm nozzle, measured with a 1 keV electron beam scanning the jet transversely (y axis) 5 mm from the nozzle tip. The nozzle was cooled to 38 K and the flow rate was 1.04×10^{20} molecules/s (corresponding to a pushing pressure of 267 mbar).

H-jet target for FNAL Main ring, P.Mansch, F.Turkot.



Dubna H-jet
internal target
with liquid Helium
cryo-pumping.



Supersonic jet target.

In case of experiments where only a low target thickness, on the order of 10^{12} atoms/cm², is desired or needed, (supersonic) gas jets, produced by the expansion of gases through fine nozzles into vacuum, are typically used. While, in principle, all gaseous target materials could be used and the target thickness would display no time structure, this type of target has the disadvantage of generating a target beam with a large geometrical divergence. In addition, the spatial target density distribution is locally homogeneous, apart from the distinct structures caused by shock fronts in the immediate vicinity of the nozzle. One major disadvantage of this type of target is that the nozzle has to be placed close to the interaction point ($\ll 1$ m) if high target densities ($\geq 10^{12}$ atoms/cm²) are required. This commonly

Introduces a high gas load to the storage ring vacuum.

Cluster jet targets.

In contrast, cluster jet targets provide a freely adjustable target thickness of up to about 10^{15} atoms/cm² [7] even at larger distances from the nozzle. They produce small nanoparticles from cooled gases or liquids via expansion in Laval-type nozzles, by either condensation of the gas or by breaking up the liquid into a spray of tiny droplets. These clusters typically consist of $10^3 - 10^6$ molecules [8, 9]. Different to pellet targets, the random nature of the cluster production introduces a homogeneous spatial distribution and no distinct time structure.

Jet target at IUCF.

J.E.Doscow,..., IUCF,
NIMA 362, 1995

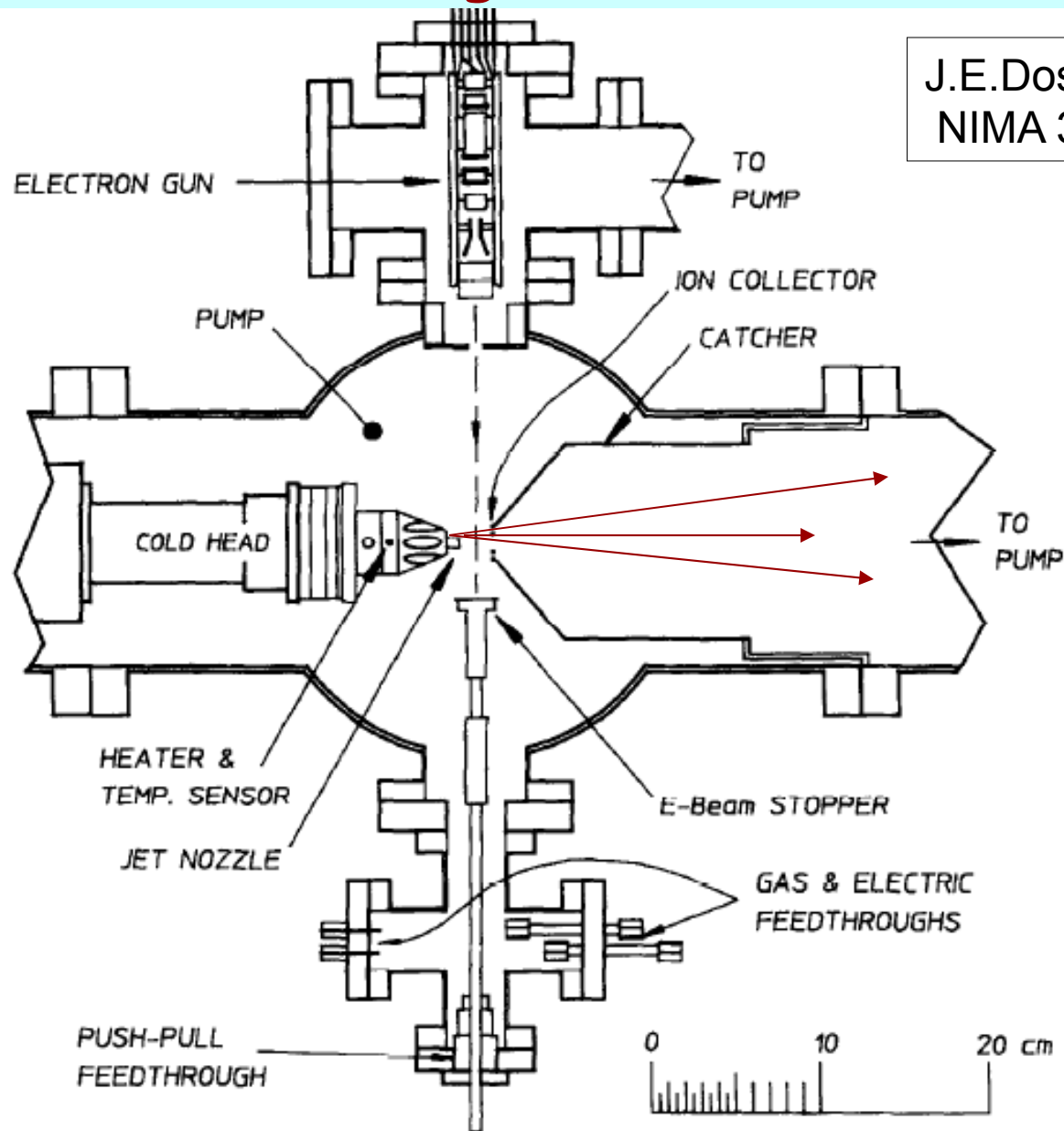


Fig. 1. Top view of the setup used to measure gas jet thickness profiles with an ionizing electron beam.

Glass nozzle geometry of the Jet target at IUCF.

J.E.Doscow,..., IUCF,
NIMA 362, 1995

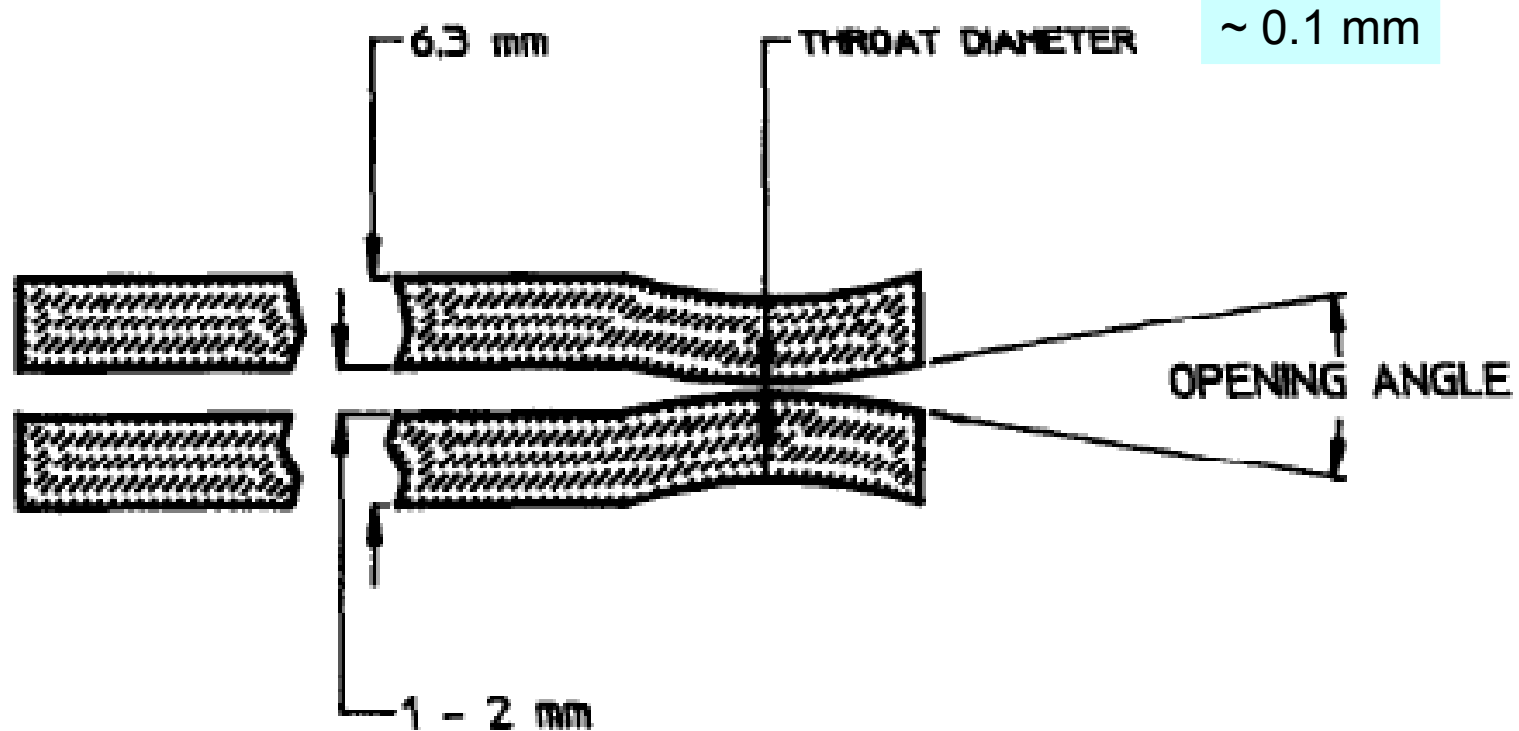


Fig. 3. Schematic drawing of glass nozzle.

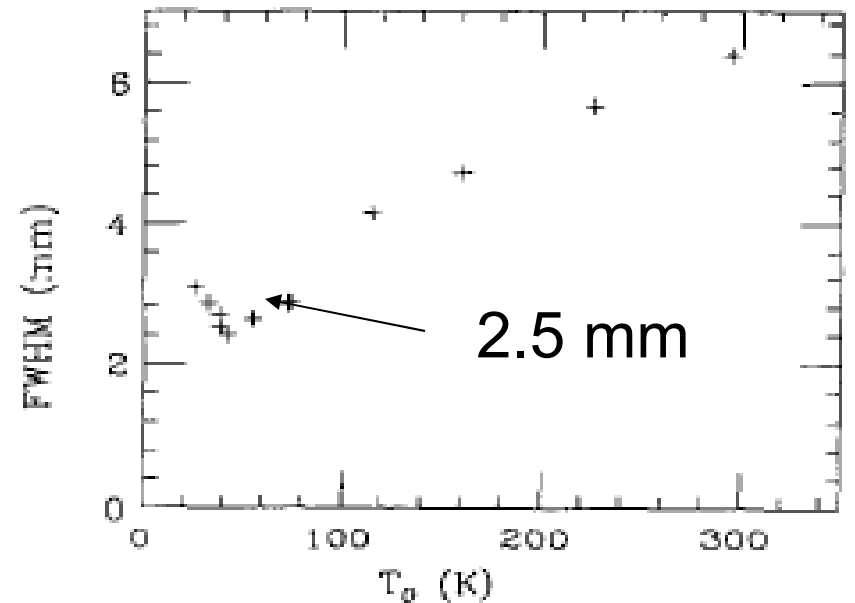
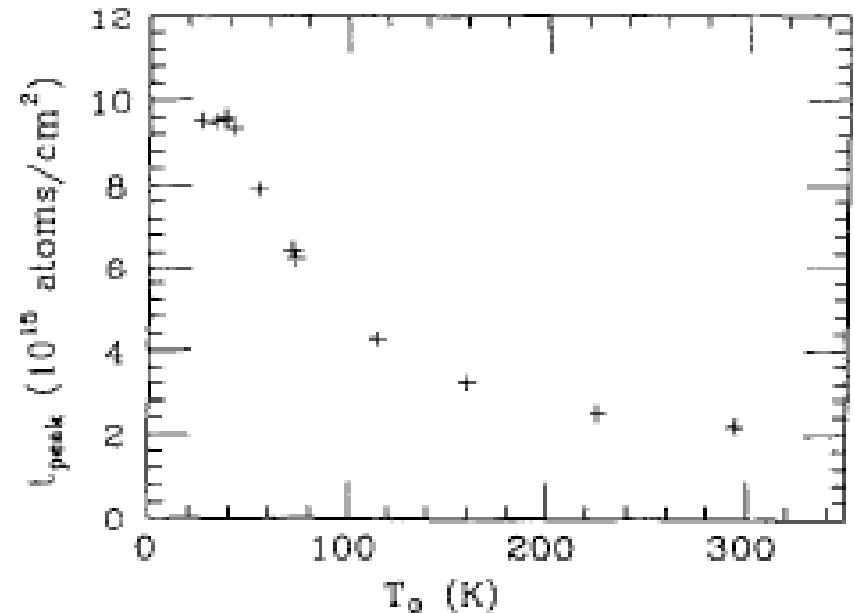
Thickness and width of the H₂-jet dependence on the nozzle jet temperature.

J.E.Doscow,..., IUCF,
NIMA 362, 1995

Temperature dependence of the H₂-jet thickness ($\times 10^{15}$ atoms/cm²).

Flow rate was $\sim 1 \cdot 10^{20}$ molecules/s.

Jet FWHM at the distance ~ 5 mm from the nozzle (vs. nozzle temperature).



Jet formation.

P.Mantcsh,. FNAL, TM-582

results of eq. (2). Measurements performed on a de Laval nozzle of throat diameter 0.1 mm gave a linear relation between the jet full width at half maximum, $2R$, and the distance Z from the nozzle. At inlet pressures above about 40 psia, Mantsch and Turkot found that for hydrogen the fwhm is independent of inlet pressure and is approximated by

$$2R = 0.16Z + 0.4, \quad (4)$$

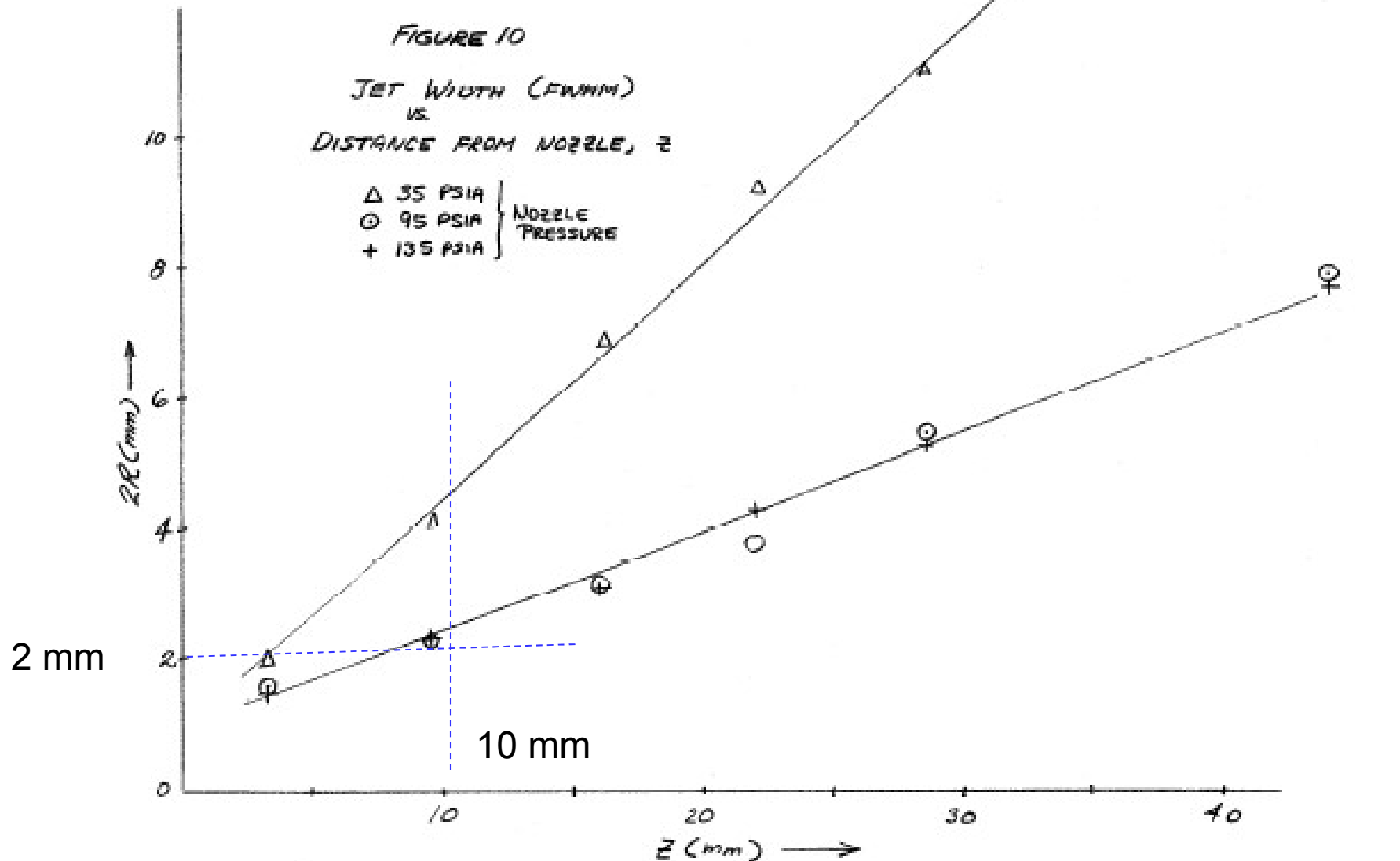
where both R and Z are in mm. At pressures below 40 psia, there is a transition to a wider profile. Measure-

ments at 35 psia give

$$2R = 0.38Z + 0.25.$$

H-jet width (2R) vs. distance from the nozzle (Z).

P.Mantcsh,. FNAL, TM-582



Gas flow through the supersonic nozzle.

5 torr-l/s \sim 6.6 scc/s
 $\sim 1.8 \cdot 10^{20}$ H₂/s

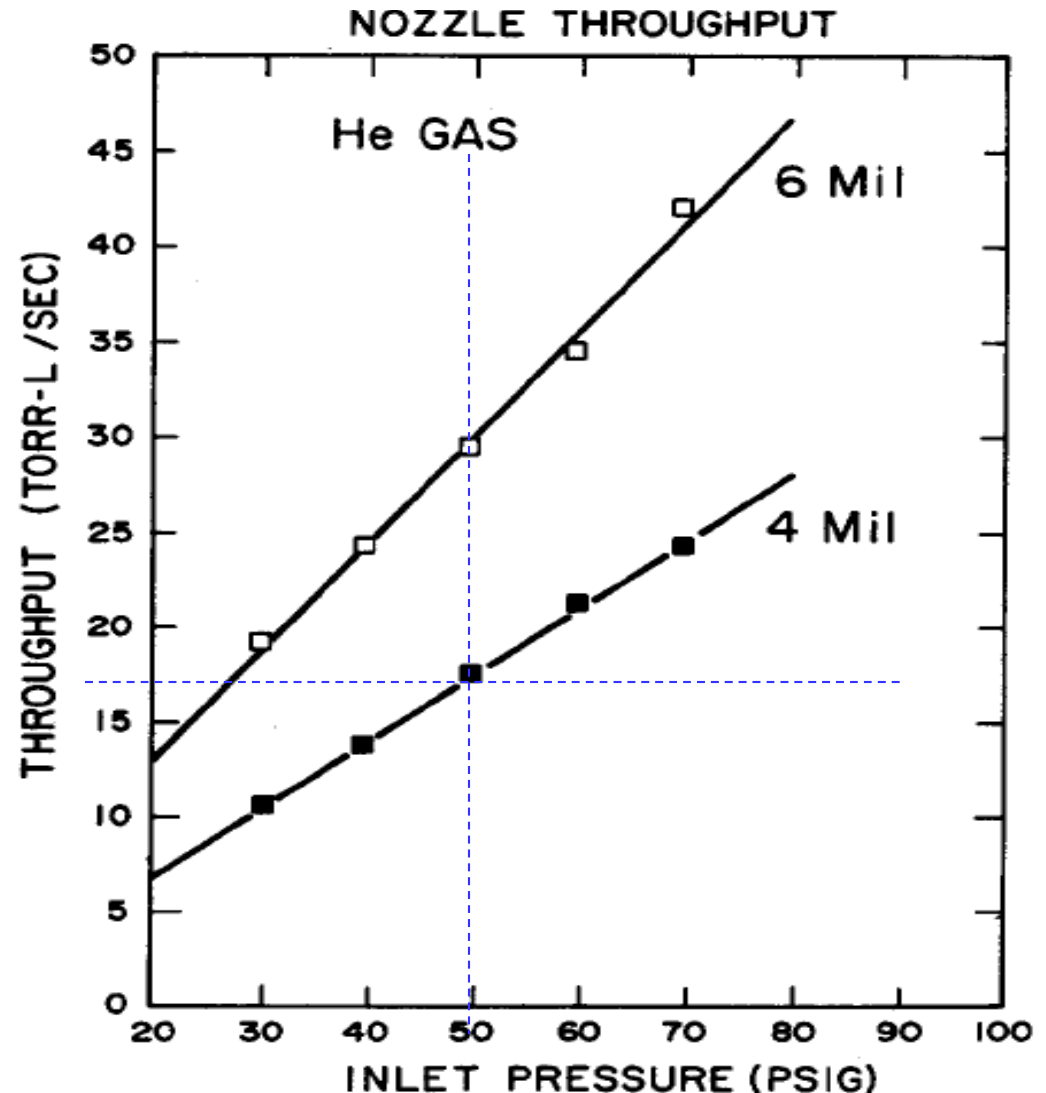


Fig. 2. Measured helium throughput of two de Laval nozzles with throat radii of 4 and 6 mil. The lines are plots of eq. (3).

B.C.Springfellow,..,NIM A251,1986

H₂ flow through 0.004" nozzle.

The H₂ gas flow through the .004" (diameter) Los Alamos nozzle for T_O = 295°K can be calculated from eq. (7) to be

$$\begin{aligned} Q &= 6.11 P_O \text{ (atm)} \frac{\text{atm} \cdot \text{cm}^3}{\text{sec}} \\ &= 4.65 P_O \text{ (atm)} \frac{\text{Torr} \cdot \ell}{\text{sec}} \end{aligned}$$

Q was measured by noting that this nozzle exponentially discharged (into a static vacuum) a 12.5 cm³ volume with a time constant of 2.05 sec.

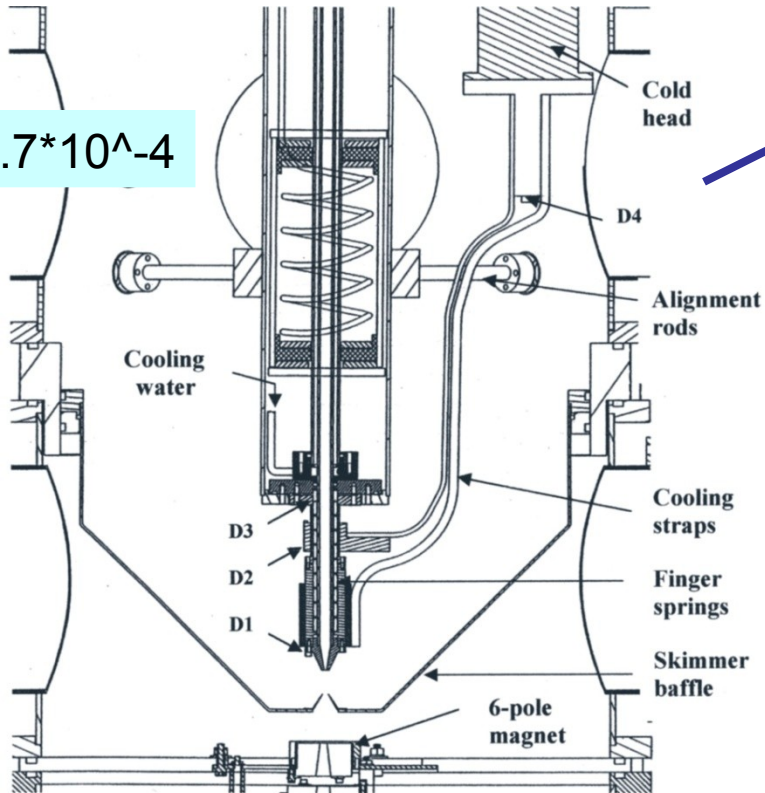
$$Q_{\text{MEASURED}} = \frac{12.5 \text{ cm}^3}{2.05 \text{ sec}} = 6.10 \frac{\text{atm} \cdot \text{cm}^3}{\text{sec}}$$

6.1 scc/sec ~ 16.5·10¹⁹ molecules/sec.

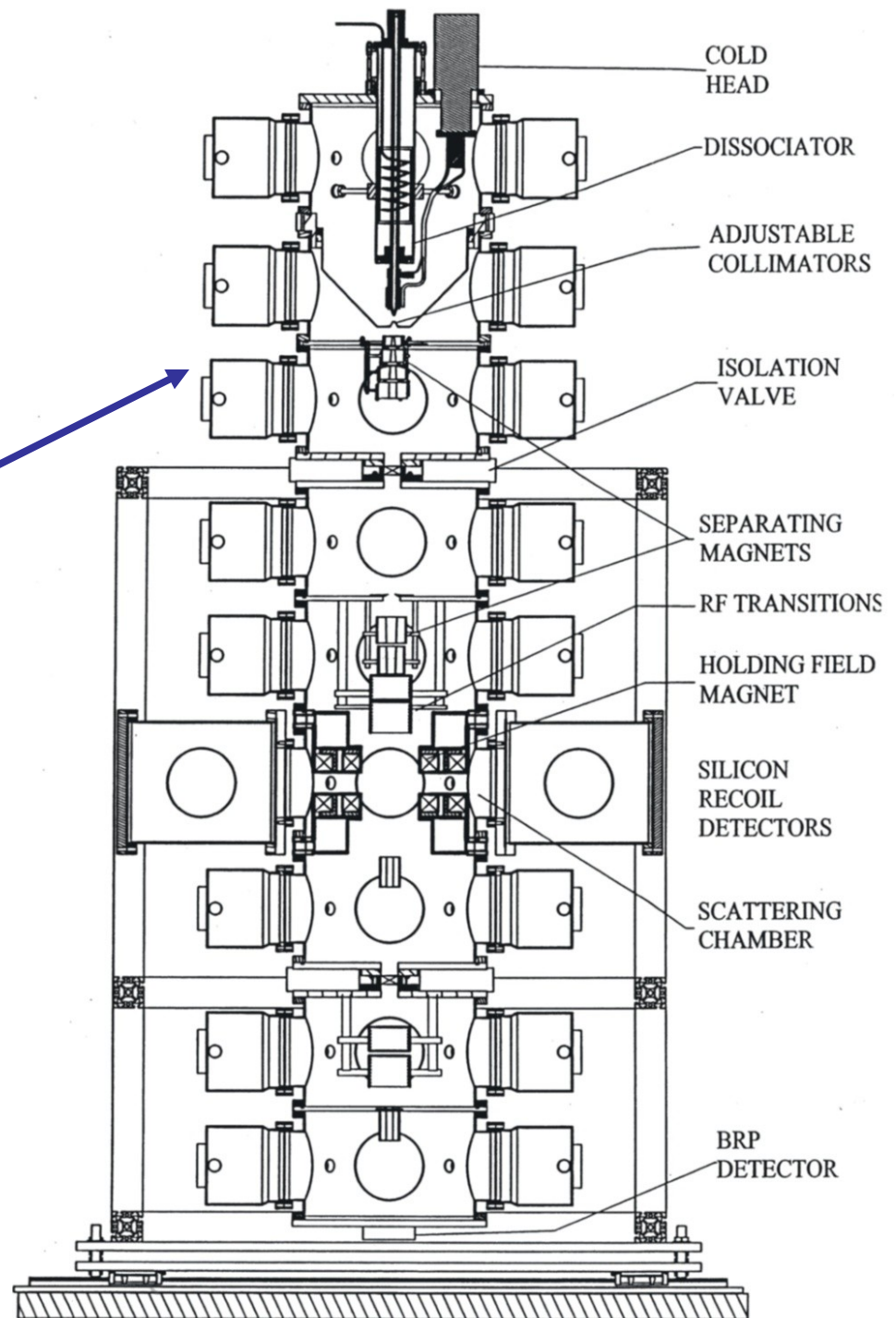
H - jet polarimeter.

2.7×10^{19} H₂/sec

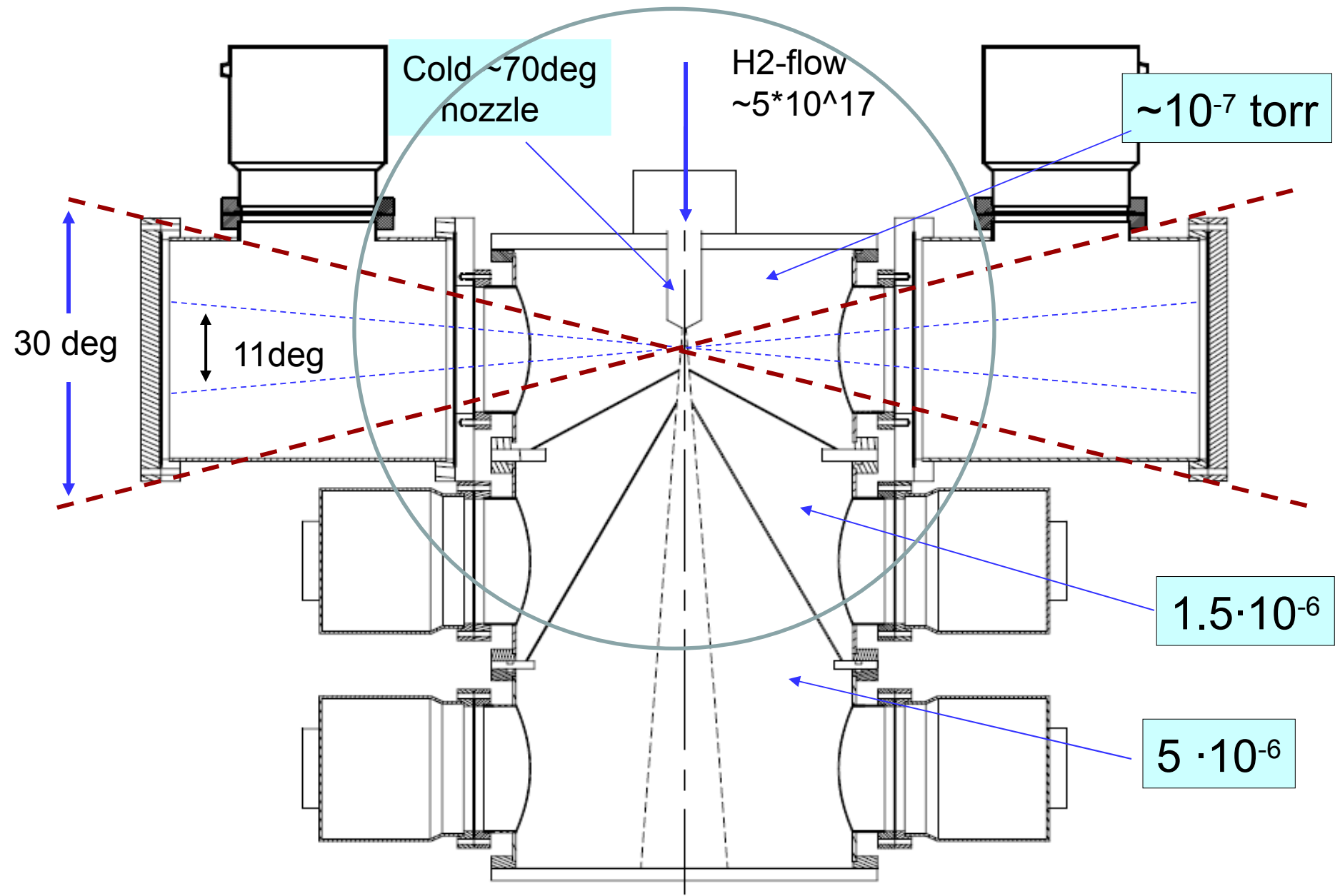
2.7×10^{-4}



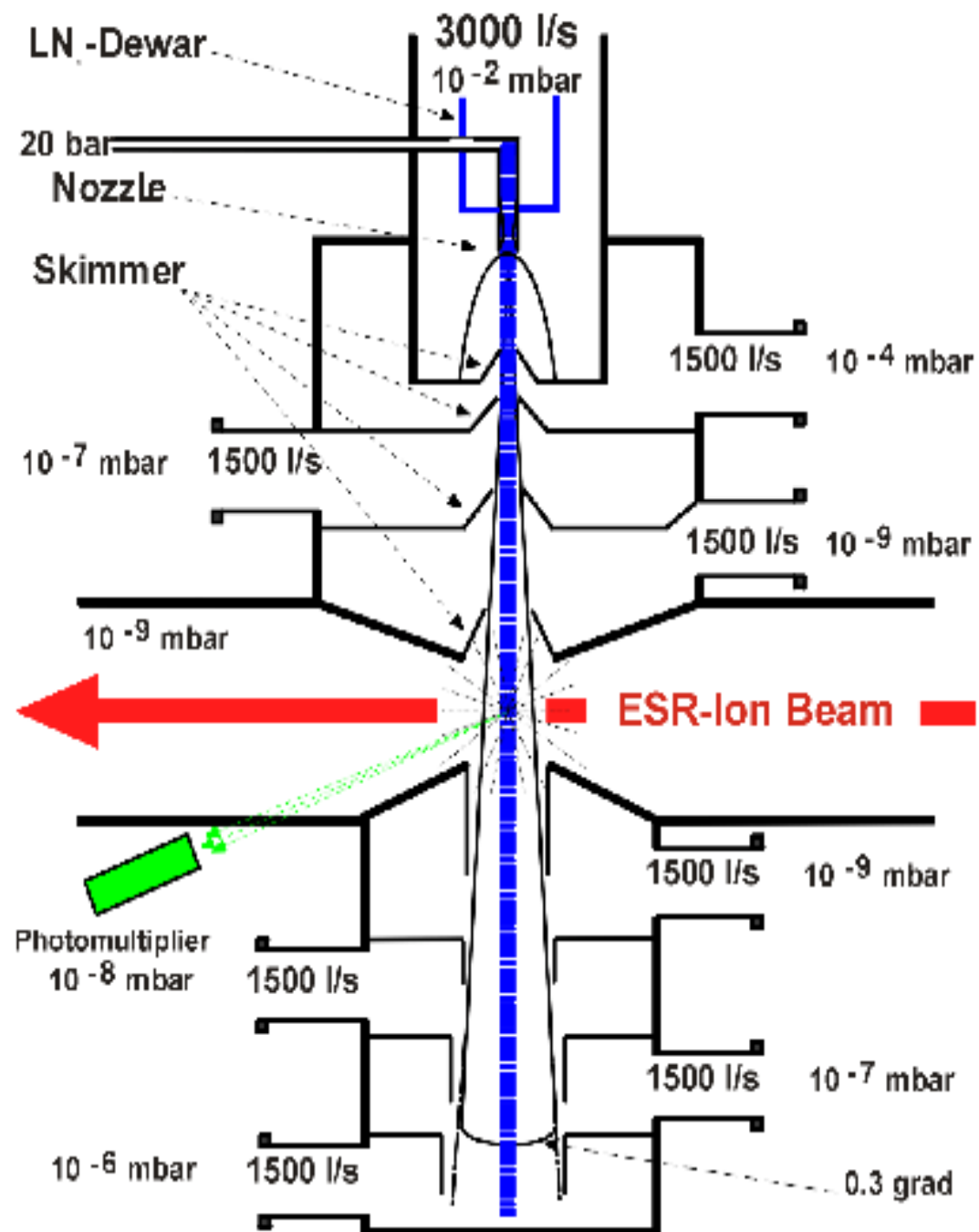
Dissociator



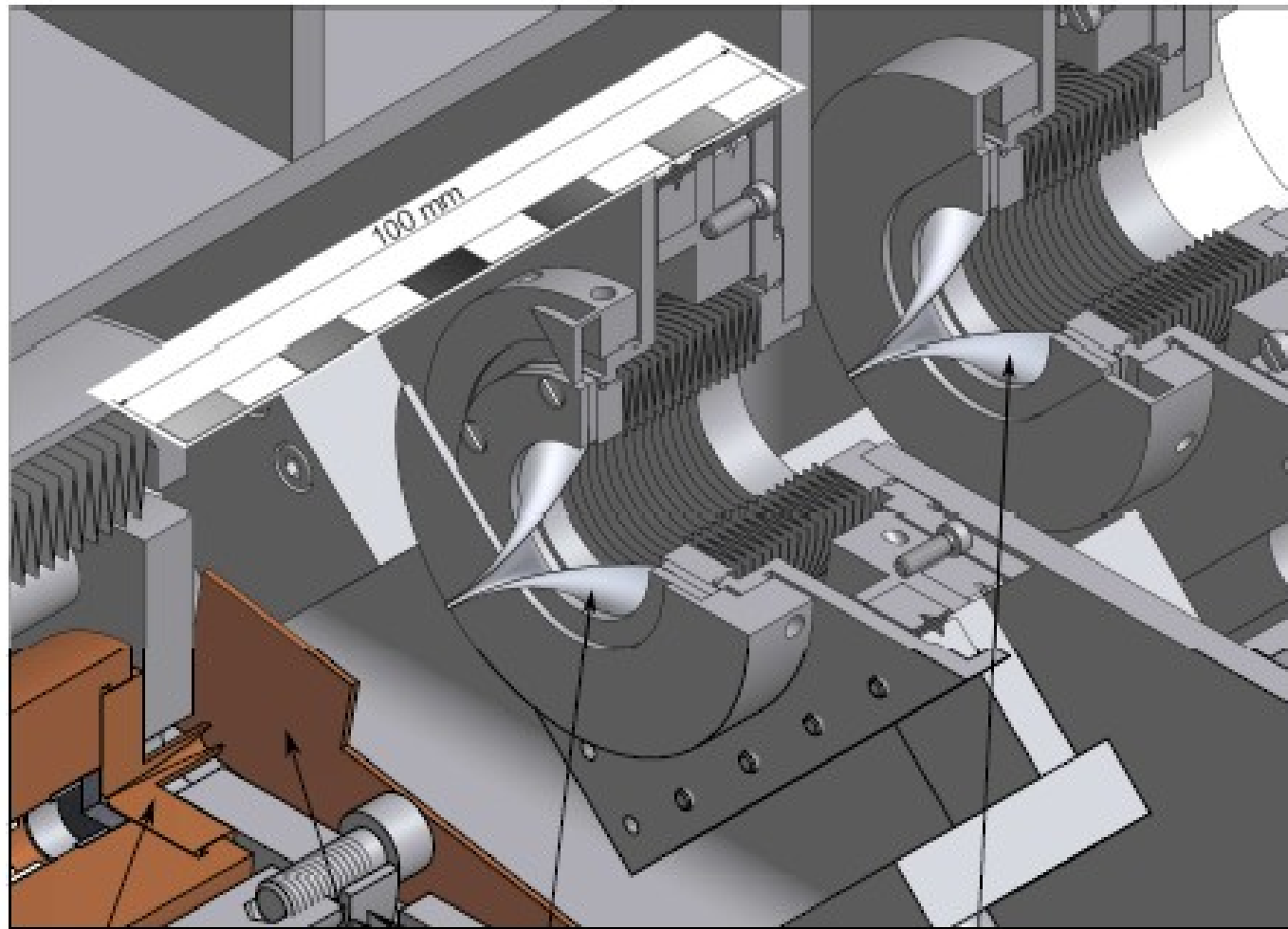
Un-polarized H₂- gas jet target.



A.Kramer,..., The
Hydrogen Cluster Target
at the ECR,
GSI Darmstadt.



A. Taschner, ... PANDA at HECR, cluster jet target
FAIR, Darmstadt.



Laval nozzle

beam

skimmer

collimator

A.Taschner,... PANDA at HECR, cluster jet target.

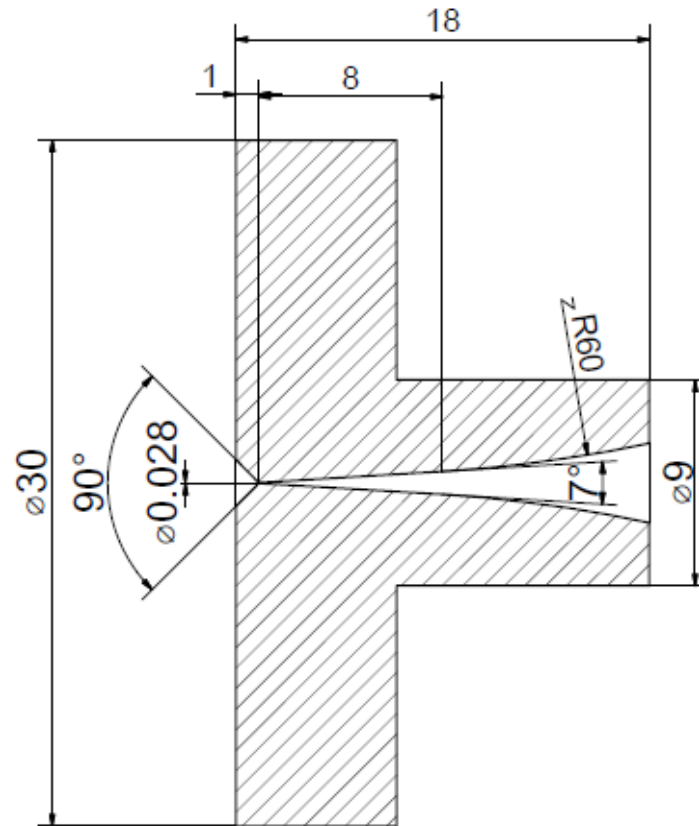


Figure 4: Cross section of the copper Laval nozzle used. This was manufactured in the CERN workshop.

Cluster-jet target density profile.

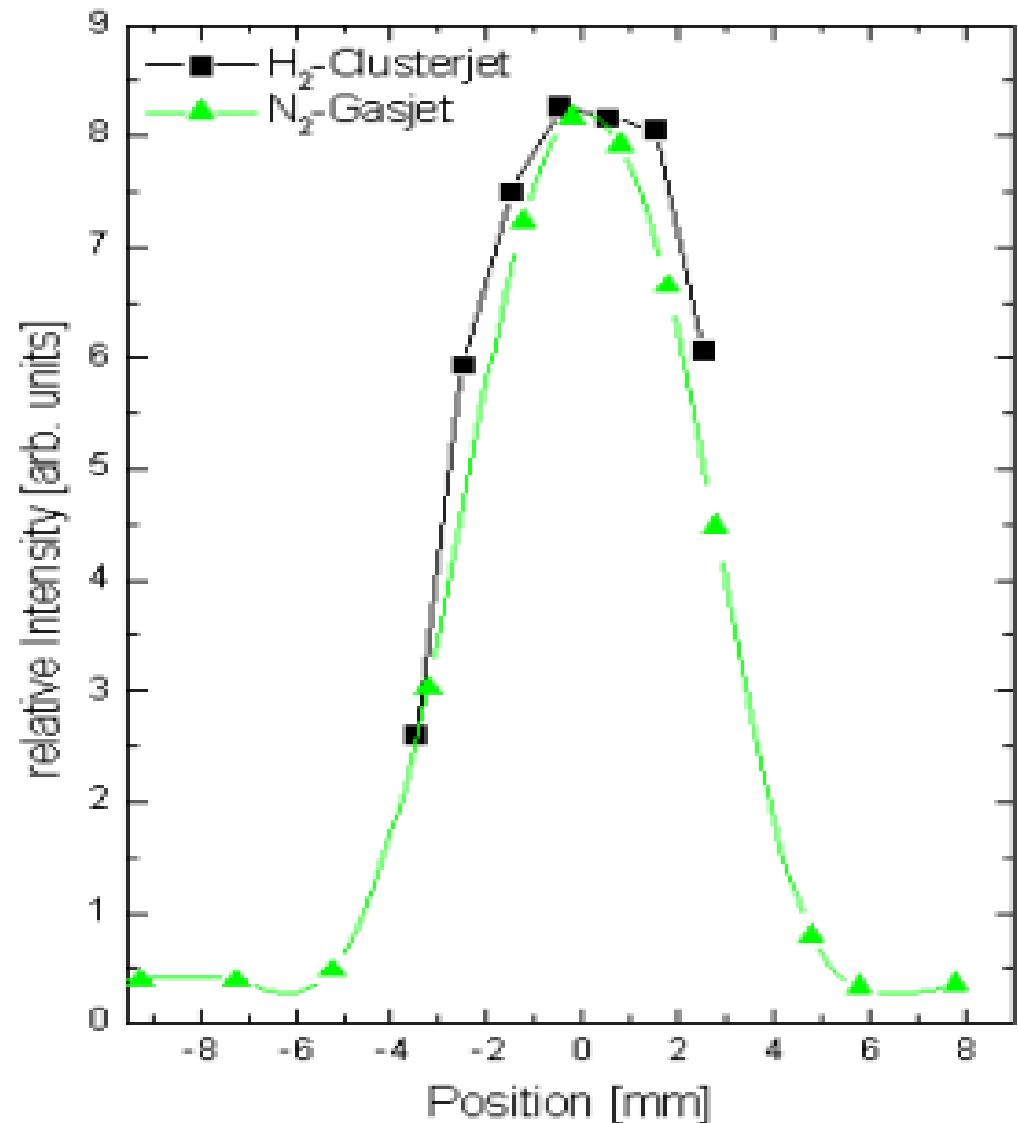


TABLE 1. Typical operation parameters of hydrogen cluster-jet targets.

	CELSIUS	E835 FERMILAB	ANKE COSY-11	Münster
nozzle diameter	100 μm	37 μm	11-16 μm	16-28 μm
gas temperature	20-35 K	20-32 K	22-35 K	20-35 K
gas pressure	1.4 bar	< 10 bar	18 bar	> 18 bar
distance from nozzle	0.32 m	0.26 m	0.65 m	2.1 m
target thickness	$1.3 \cdot 10^{14} \text{ cm}^{-2}$	$3 \cdot 10^{14} \text{ cm}^{-2}$	$> 10^{14} \text{ cm}^{-2}$	$> 4 \cdot 10^{14} \text{ cm}^{-2}$

A.Gruber,... Internal gas-jet target for the ECR at GSI, NIM A282 (1989).

Stage no.	Pressure [Pa]	Molecular density [cm ⁻³]	Pumping speed [l/s]	Gas consumption [Pa l/s]	Skimmer, radius [mm]
<i>Injection system</i>					
1	5	2.5×10^{16}	3000	15 000	0.25
2	5×10^{-4}	1.9×10^{15}	1500	0.4	0.92
3	9×10^{-7}	4.2×10^{14}	1500	2×10^{-4}	1.58
4	7×10^{-9}	1.8×10^{14}	1500	1×10^{-6}	2.25
<i>ESR</i>					
	1×10^{-9}	1×10^{14}	—	5×10^{-8}	2.4
<i>Jet dump</i>					
4	3×10^{-9}	4.5×10^{13}	1500	4×10^{-6}	2.6
3	1×10^{-6}	1.6×10^{13}	1500	1×10^{-3}	5.1
2	3×10^{-4}	8.4×10^{12}	1500	0.4	7.6
1	2×10^{-2}	5.1×10^{12}	1500	20	10.1

Towards precision polarimetry in RHIC. Summary.

- Analyzing power of P-P elastic scattering in CNR region has been accurately measured in experiments with H-jet polarimeter in energy range 24-250 GeV.
- This accuracy can be further improved after studies of molecular H₂ background and other systematic errors contributions.
- The known analyzing power can be used in the polarimeter with higher thickness un-polarized H₂-jet target and 100 times higher counting rate.
- This will result in less than 1% statistical accuracy for each fill.
- Tenfold rate increase can be obtained due to Jet geometry optimization and detector solid angle increase.
- In this assumption, the required H₂-jet target thickness will be about:
$$(5-10) \cdot 10^{12} \text{ H}_2 \text{ molecules /cm}^2.$$
- This target thickness can be achieved in comparatively simple H₂-jet target.
- The effect of this Jet-target to the beam and RHIC vacuum will be small (comparable with the polarized H₂-jet target).

A.Taschner,... PANDA at HECR, cluster jet target.

pumping stage	pumps	typical pressure
insulation vacuum chamber	turbo pump: 370 l/s (Leybold Turbovac 361)	10^{-5} mbar
skimmer chamber	roots pump: 3000 m ³ /h (Leybold Ruvac RA3001) roots pump: 2000 m ³ /h (Leybold Ruvac WSL2001)	8×10^{-2} mbar
collimator chamber	turbo pump: 2×900 l/s (Leybold Turbovac 1000 C)	2×10^{-4} mbar
cryopump stage	Münster type cryopump	2×10^{-5} mbar
intermediate stage	turbo pump: 110 l/s (Leybold Turbovac 150)	10^{-5} mbar
scattering chamber	turbo pump: 340 l/s (Leybold Turbovac 360)	3×10^{-5} mbar
1st beam dump	Münster type cryopump	6×10^{-6} mbar
2nd beam dump	turbo pump: 900 l/s (Leybold Turbovac 1000 C) turbo pump: 370 l/s (Leybold Turbovac 361 C)	7×10^{-6} mbar
3rd beam dump	Münster type cryopump	3×10^{-5} mbar
4th beam dump	turbo pump: 900 l/s (Leybold Turbovac 1000 C)	8×10^{-5} mbar

Table 2: Vacuum pumping system of the cluster jet target with pressures for operation at highest target thickness and therefore highest gas flow through the nozzle.

A.Gruber,... Internal gas-jet target for the ECR at GSI, NIM A282 (1989).

Table 1

Parameters of the internal target using hydrogen with $P_0 = 1 \times 10^6$ Pa, $T_0 = 200$ K, nozzle neck radius $r_n = 0.07$ mm and nozzle exit radius $r_e = 2$ mm

Stage no.	Pressure [Pa]	Molecular density [cm^{-3}]	Pumping speed [l/s]	Gas consumption [Pa l/s]	Skimmer/pipe radius [mm]	Pipe length [mm]	Flow conductance [l/s]
<i>Injection system</i>							
1	5	2.5×10^{16}	3000	15 000	0.25	–	0.09
2	5×10^{-4}	1.9×10^{15}	1500	0.4	0.92	–	0.12
3	9×10^{-7}	4.2×10^{14}	1500	2×10^{-4}	1.58	–	3.50
4	7×10^{-9}	1.8×10^{14}	1500	1×10^{-6}	2.25	–	7.09
<i>ESR</i>							
	1×10^{-9}	1×10^{14}	–	5×10^{-8}	2.4	–	–
<i>Jet dump</i>							
4	3×10^{-9}	4.5×10^{13}	1500	4×10^{-6}	2.6	200	0.33
3	1×10^{-6}	1.6×10^{13}	1500	1×10^{-3}	5.1	200	2.48
2	3×10^{-4}	8.4×10^{12}	1500	0.4	7.6	200	8.19
1	2×10^{-2}	5.1×10^{12}	1500	20	10.1	200	19.23

A.Gruber,... Internal gas-jet target for the ECR at GSI, NIM A282 (1989).

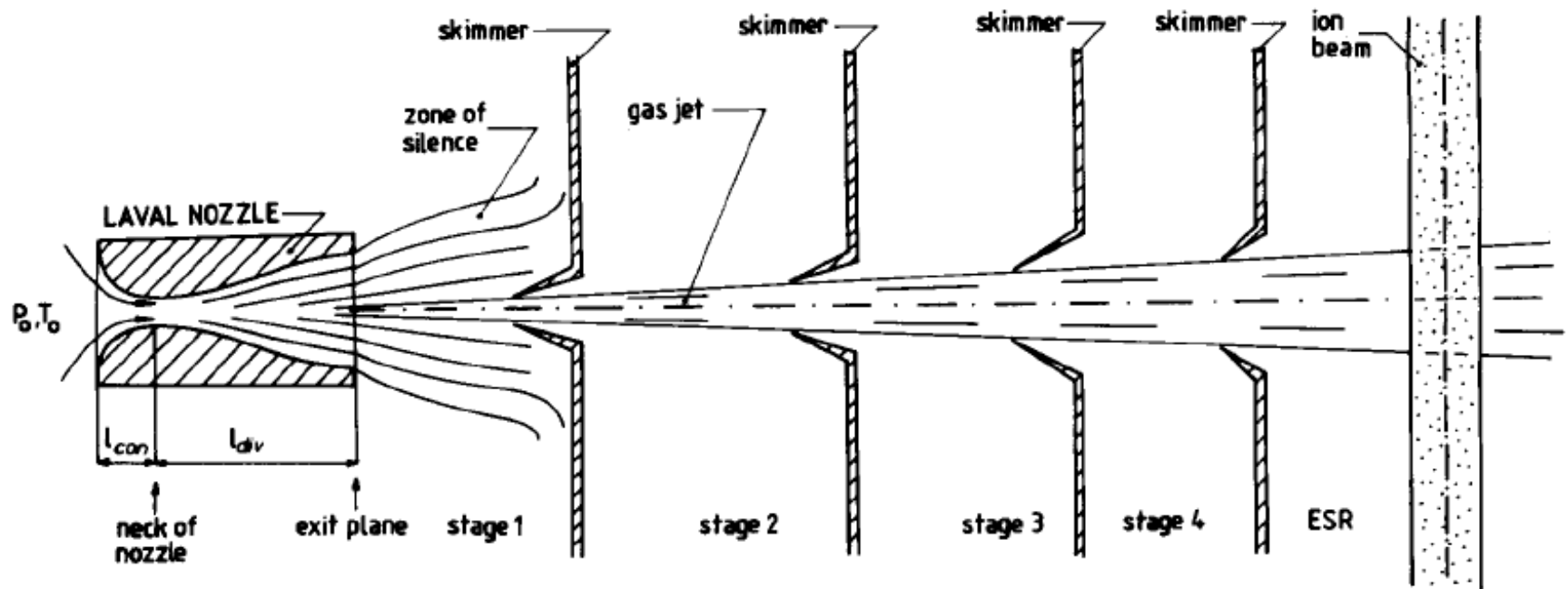


Fig. 1. Principal sketch of the gas jet production or injection system showing the lengths of the converging (l_{con}) and diverging (l_{div}) part of the nozzle as well as the flow lines and the "zone of silence". Corresponding pressures and jet densities in stages 1–4 and nozzle geometry data are listed in table 1.

8.1 Accomplishments with the Los Alamos 0.004"-Diameter Nozzle

A test bench gas jet target using the Los Alamos de Laval was set up and run with H_2 gas at room temperature (295°K). In addition to the nozzle, the basic components of the system were: (a) a 10" oil diffusion pump, (b) a 4" oil diffusion pump, and (c) a three-solenoid system for generating a square jet pulse. With this simple system, we were able to make a prototype target that had the capabilities to:

- (1) run continuously with 100-msec long pulses spaced by 1 sec;¹⁴
- (2) give a 5 mm wide jet (FWHM) at 2.5 cm from the nozzle tip;
- (3) vary ρl over the range $0.3 - 3 \times 10^{-8} \text{ g/cm}^2$;
- (4) yield a ratio of background gas density to jet of 1/200;
- (5) transmit 86% of the directed jet gas through a 3.8 cm diameter hole 5.1 cm below the nozzle tip.